The Journal of Engineering Research Vol. 6, No. 2 (2009) 20-32

Effect of Material Parameters on Steady State Creep in a Thick Composite Cylinder Subjected to Internal Pressure

Tejeet Singh[a] and V.K.Gupta[*b]

[a]*Department of Mechanical Engineering, S. B.S. College of Engineering and Technology, Ferozepur, 152001, India*
[*b] *Department of Mechanical Engineering, University College of Engineering, Punjabi University, Patiala-147002, India*

Received 25 April 2008; accepted 26 October 2008

تأثير عوامل المادة على الزحف المنتظم لإسطوانة مركبة سميكة معرضة لضغط داخلي

تيجات سنج و ك. جوبتا×

الخلاصة : تم دراسة الزحف المنتظم لأسطوانة مركبة معرضة لضغط داخلي. إن سلوك زحف المادة قد تم وصفها على أساس قوة الاجهاد المبنية على قانون الزحف بإفتراض أس الإجهاد مساويا خمسة. هذا وقد تم دراسة تأثير عامل الحجم ومحتوى التقوية ودرجة حرارة التشغيل على معدلات الاجهاد و الاستطالة بالاسطوانة المركبة. وقد أشارت الدراسة الى ان الإجهادات بالاسطوانة لا تتقيد بشكل معزز مع تغيرات ومحتوى التقوية ودرجة حرارة التشغيل. ومع ذلك فقد وجد أن معدلات الأجهاد المماسية و القطرية للإسطوانة تقل الى حد ملحوظ عند تقليل الحجم و زيادة المحتوى و تقليل درجة حرارة التشغيل.

المفردات المفتاحية : اسطوانة، زحف، مركب، ضغط داخلى، نمذجة.

Abstract: The steady state creep in Al- SiC_P composite cylinder subjected to internal pressure was investigated. The creep behavior of the material were described by threshold stress based creep law by assuming a stress exponent of 5. The effect of size and content of the reinforcement (SiC_P), and operating temperature on the stresses and strain rates in the composite cylinder were investigated. The stresses in the cylinder did not have significant variation with varying size and content of the reinforcement, and operating temperature. However, the tangential as well as radial strain rates in the cylinder could be reduced to a significant extent by decreasing size of SiC_P, increasing the content of SiC_P and decreasing operating temperature.

Keywords: Cylinder, Creep, Composite, Internal pressure, Modeling

1. Introduction

Cylinder made of monolithic material such as metal and concrete (*eg*. asphalt concrete), is a common component employed in numerous applications such as pressure vessels (*eg*. hydraulic cylinders, gun barrels, pipes, boilers and fuel tanks), accumulator shells, emergency breathing cylinders, cylinders for aerospace industries, nuclear reactors, military applications and civil structures etc. (Arya, Bhatnagar, 1976; Bhatnagar, *et al*. 1980; Becht, *et al*. 2000; Gupta, *et al*. 2001; Perry and Aboudi, 2003; Buttlar, *et al*. 2004 and You and Buttlar, 2005). In some of these applications such as pressure vessel for industrial gases or a media transportation of high-pressurized fluids and piping of nuclear reactors, the cylinder has to operate under severe mechanical and thermal loads, causing significant creep hence reduced service life (Gupta and Pathak, 2001; Tachibana and Iyoku, 2004 and Hagihara and Miyazaki, 2008). As an example, in the high temperature engineering test reactor, the temperature reaches of the order of 900 ^{0}C (Tachibana and Iyoku, 2004). The piping of reactor cooling system is subjected to high temperature and pressure and may be damaged due to high heat generated from the reactor core (Hagihara and Miyazaki, 2008).

Creep analysis of thick-walled cylinder made of isotropic monolithic material and subjected to internal pressure has been presented by (Weir, 1957; King and Mackie 1967 and Pai 1967) has solved the problem for orthotropic cylinders. In all these analyses it was assumed that the strains are infinitesimal and the deformation is referred with respect to original dimensions of the cylinder. Rimrott, 1959, used generally accepted assumptions of constant density, zero axial strain and distortion energy theory to derive equations for creep rate, creep strains and creep stresses in a, closed end, thick-walled hollow cylinder subjected to internal pressure. Bhatnagar and Gupta, 1969 obtained the solution for thick walled cylinder made of an orthotropic material and subjected to internal pressure. In recent years, the problem of creep in composite cylinders made of Functionally Graded Materials (FGMs) operating at high pressure and temperature has attracted the interest of many researchers. Fukui and Yamanaka, 1992 investigated the effect of gradation of components on strength and deformation of thick-walled Functionally Graded (FG) tubes subjected to internal pressure under

*Corresponding author's e-mail: guptavk_70@yahoo.co.in

plain strain conditions. Fukui *et al*. 1993 extended the work to investigate the effect of graded components on residual stresses in a thick walled FG tube under uniform thermal loading. Chen *et al*. 2007 studied the creep behavior of a thick walled FGM cylinder subjected to internal and external pressures. The asymptotic solutions were obtained on the basis of Taylor expansion series and compared with the results obtained by finite element analysis. You *et al*. 2007 investigated steady state creep in a thick walled FGM cylinder subjected to internal pressure. The effect of variation in material parameters on the stresses induced in cylinder was investigated. Abrinia *et al*. 2008 obtained the analytical solution for radial and circumferential stresses in a thick FGM cylindrical vessel under the influence of internal pressure and temperature. The study indicated that stresses in FGM cylinder could be lowered by tailoring the material properties along radial direction of the cylinder.

Under severe thermo-mechanical loads cylinder made of monolithic materials may not perform well. The metal matrix composites (MMCs) such as aluminium/aluminium alloy matrix reinforced with silicon carbide offer excellent mechanical properties like high specific strength and stiffness along with high temperature stability. Therefore, these are suitable for cylinder applications exposed to high pressure and high operating temperature (Nieh, 1984; Roy and Tsai, 1988; Fukui *et al*. 1993; Salzar *et al*. 1996 and Gupta *et al*. 2004. With these forethoughts, it is decided to investigate the steady state creep in a cylinder made of Al- SiC_P composite and subjected to high pressure and high temperature. A mathematical model has been developed to describe the steady creep behavior of the composite cylinder. The model developed is used to investigate the effect of material parameters viz particle size and particle content, and operating temperatures on the steady state creep response of the composite cylinder.

2. Selection of Creep Law

In aluminium based composites, undergoing steady state creep, the effective creep rate, $\dot{\varepsilon}_e$, is related to the effective stress, σ_e, through well documented threshold stress, σ_0, based creep law given by (Mishra and Pandey, 1990; Pandey *et al*. 1992; Gonzalez-Doncel and Sherby, 1993; Pandey *et al*. 1994; Park *et al*. 1990; Mohamed *et al*. 1992; Part and Mohamed, 1995; Cadek *et al*. 1995; Yoshioka *et al*. 1998; Li and Mohamed, 1997; Li and Langdon, 1997; Li and Langdon, 1997; Li and Langdon, 1999; Tjong and Ma 2000 and Ma and Tjong, 2001).

$$\dot{\varepsilon}_e = A'\left(\frac{\sigma_e - \sigma_0}{E}\right)^n exp\left(\frac{-Q}{RT}\right) \tag{1}$$

where the symbols A', n, Q, E, R and T denote respectively structure dependent parameter, true stress exponent, true activation energy, temperature-dependent Young's modulus, gas constant and operating temperature.

The true stress exponent n appearing in Eq. (1) is usually selected as 3, 5 and 8 which correspond to three well-documented creep cases for metals and alloys: (i) $n = 3$ for creep controlled by viscous glide processes of dislocation, (ii) $n = 5$ for creep controlled by high temperature dislocation climb (lattice diffusion), and (iii) $n = 8$ for lattice diffusion-controlled creep with a constant structure (Tjong and Ma, 2000). Though, some of the research groups (Mishra and Pandey, 1990; Pandey *et al*. 1992; Gonzalex-Doncel and Sherby, 1993 and Pandey *et al*. 1994) have used a true stress exponent of 8 to describe steady state creep in Al-$SiC_{P,W}$ (subscript '*p*' for particle and '*w*' for whisker) composites but a number of other research groups (Park *et al*. 1990; Mohamed *et al*. 1992; Park and Mohamed, 1995; Cadek *et al*. 1995; Yoshioka *et al*. 1998; Li and Mohamed, 1997; Li and Langdon, 1997 and Li and Langdon, 1999) have observed that a stress exponent of either ~3 or ~5, rather than 8, provides a better description of steady state creep data observed for discontinuously reinforced Al-SiC composites. Keeping this in view, a stress exponent of 5 is used to describe steady state creep behavior of the composite cylinders in this study. The justification regarding choice of stress exponent is further elaborated in the next section.

3. Estimation of Creep Parameters

The creep law given by Eq. (1) may alternatively be written as:

$$\dot{\varepsilon}_e = \left[M\left(\sigma_e - \sigma_0\right)\right]^n \tag{2}$$

where $M = \frac{1}{E}\left(A' exp\frac{-Q}{RT}\right)^{1/n}$ and the stress exponent n is chosen as 5.

The creep parameters M and so appearing in Eq . (2) are dependent on the type of material and are also affected by the temperature (T) of application. In a composite, the dispersoid size (P) and the content of dispersoid (V) are the primary material variables determining these parameters. In the present study, the values of M and σ_0 have been extracted from the experimental creep results reported for Al -SiCP composite under uniaxial loading (Pandey *et al*. 1992). Though, Pandey *et al*. 1992 suggested a stress exponent of 8 to describe steady state creep in these composites . But due to the objections pointed by several research groups (Park *et al*. 1990; Mohamed *et al*. 1992; Park and Mohamed, 1995; Cedek *et al*. 1995; Yoshioka *et al*. 1998; Li and Mohamed, 1997; Li and Longdon, 1997 and Li and Langdon, 1999), we have used a stress exponent of 5 to describe steady state creep in composite (Al-SiCP) taken in the study of (Pandey *et a*l. 1992). The individual set of creep data of (Pandey *et al*. 1992) have been plotted as $\dot{\varepsilon}^{1/5}$ versus σ on linear scales as shown in Figs. 1(a)-(c). From the slope and intercepts of these graphs, the values of creep parameters M and σ_o have been obtained and are reported in Table-1. This approach of determining the threshold stress σ_o, is known as linear extrapolation technique (Lagneborg and Bergman, 1976). To avoid variation due to systematic error, if any, in experimental results, the creep results from a single source have been used.

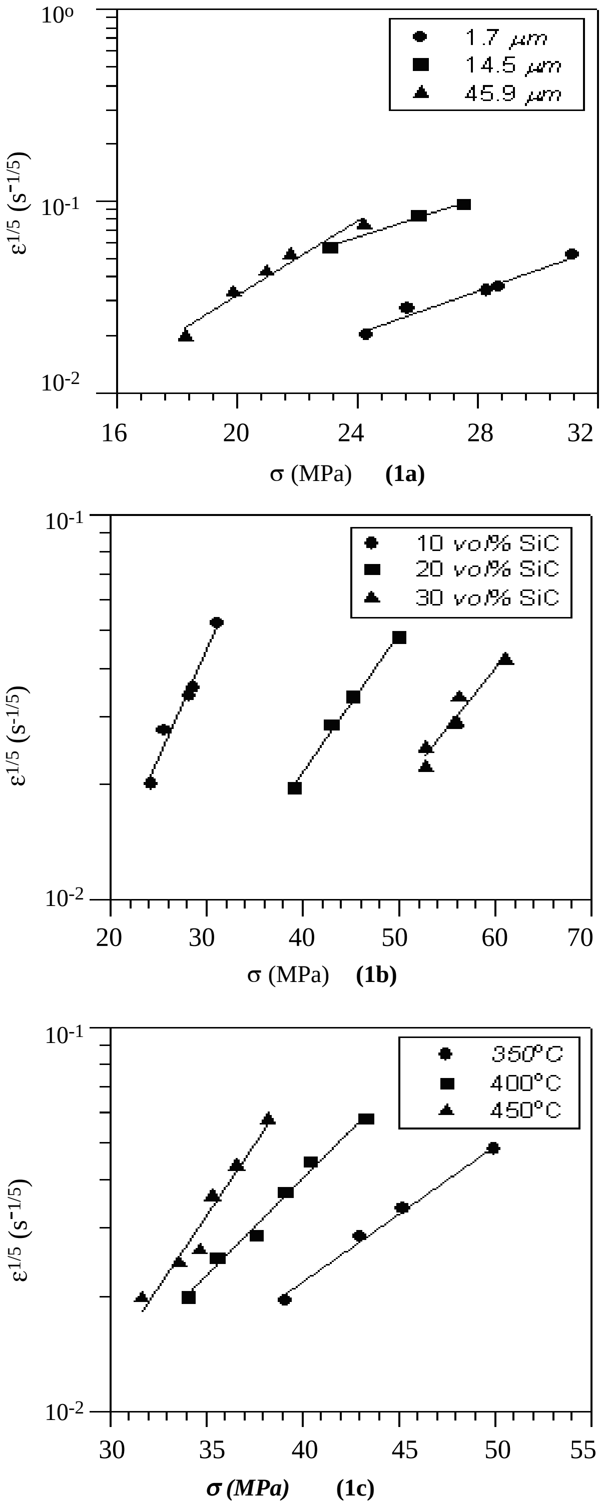

Figure 1. Variation of $\varepsilon^{1/5}$ versus σ in Al-SiC_p composite for different (a) particle sizes of SiC, (b) *vol%* of SiC and (c) temperature

The $\varepsilon^{1/5}$ versus σ plots corresponding to the observed experimental data points of Al- SiC_P composites (Pandey *et al*. 1992) for various combinations of particle size, particle content and operating temperature exhibit an excellent linearity as evident from Figs.1(a)-(c). The coefficient of correlation for these plots has been reported in excess to 0.916 as given in Table-1. In the light of these results, the choice of stress exponent $n = 5$, to describe the steady state creep behavior of Al-SiC_P composite, is justified.

The accuracy of the creep response of the composite cylinder, to be estimated in subsequent sections, will depend on the accuracy associated with prediction of creep parameters M and σ_o for various combinations of material parameters and operating temperature. To accomplish this task, the creep parameters given in Table-1 have been substituted in the constitutive creep model, Eq. (2), to estimate the strain rates corresponding to the experimental stress values reported by (Pandey *et al*. 1992) for Al-SiC_P composite for the various combinations of material parameters and temperature as given in Table-1. The estimated strain rates have been compared with the strain rates observed experimentally by (Pandey *et al*. 1992). Figs. 2(a)-(c) show an excellent agreement between the strain rates estimated from Eq. (2) and those observed experimentally, to inspire confidence in the creep parameters estimated in this study.

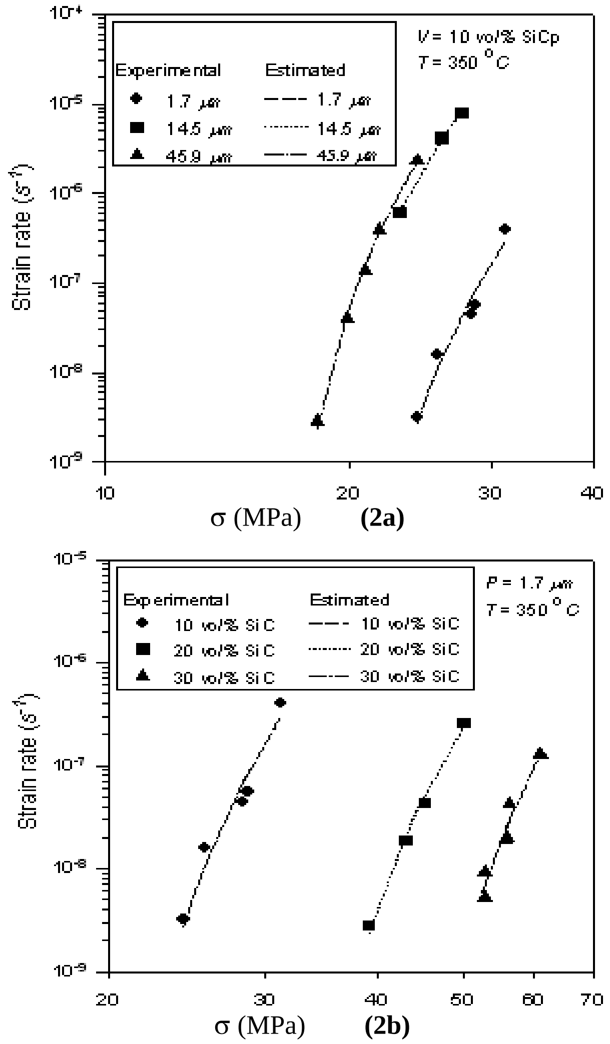

The Journal of Engineering Research Vol. 6, No. 2 (2009) 20-32

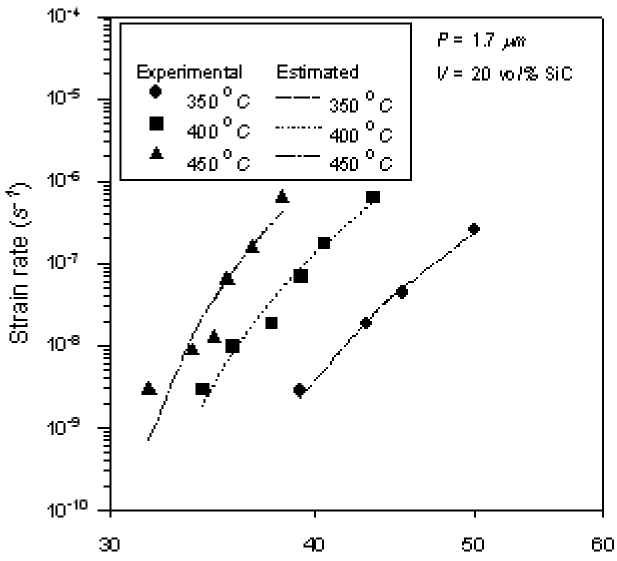

(2c)

Figure 2. Comparison of experimental and estimated strain rates in Al-SiC$_p$ composite for different (a) particle sizes of SiC, (b) *vol%* of SiC and (c) temperature

Table 1. Creep parameters used for Al-SiC$_p$ composites in the present study

P (*μm*)	**T (^0C)**	**V (*Vol %*)**	**M (*$s^{-1/5}$/MPa*)**	**σ_0 (*MPa*)**	**Coefficient of correlation**
1.7			4.35E-03	19.83	0.945
14.5	350	10	8.72E-03	16.50	0.999
45.9			9.39E-03	16.29	0.998
		10	4.35E-03	19.83	0.945
1.7	350	20	2.63E-03	32.02	0.995
		30	2.27E-03	42.56	0.945
	350		2.63E-03	32.02	0.995
1.7	400	20	4.14E-03	29.79	0.974
	450		5.92E-03	29.18	0.916

4. Mathematical Formulation

Consider a long, closed end, thick-walled hollow cylinder made of Al-SiC$_P$ composite having inner and outer radii of a and b respectively and subjected to internal pressure p. The coordinates axes r, θ and z are taken respectively along radial, tangential and axial directions of the cylinder. The present analysis is based on the following assumptions:

i. Material of the cylinder is incompressible, isotropic and has uniform distribution of SiC$_P$ in aluminium matrix.
ii. Pressure is applied gradually and held constant during the loading history.
iii. Stresses at any point in the cylinder remain constant with time *ie*. steady state condition of stress is assumed.
iv. Elastic deformations are small and are neglected as compared to creep deformations.

The radial ($\dot{\varepsilon}_r$) and tangential ($\dot{\varepsilon}_\theta$) strain rates in the cylinder are respectively given by:

$$\dot{\varepsilon}_r = \frac{d\dot{u}_r}{dr} \tag{3}$$

$$\dot{\varepsilon}_\theta = \frac{\dot{u}_r}{r} \tag{4}$$

where $\dot{u}_r = \dfrac{du}{dt}$ is the radial displacement rate and u is the radial displacement.

$$r\frac{d\dot{\varepsilon}_\theta}{dr} = \dot{\varepsilon}_r - \dot{\varepsilon}_\theta \tag{5}$$

Considering the equilibrium of forces on an element of the cylinder in the radial direction, we may write, (Gupta and Pathak, 2001)

$$r\frac{d\sigma_r}{dr} = \sigma_\theta - \sigma_r \tag{6}$$

where σ_θ is the tangential stress.

Since material of the cylinder is assumed to be incompressible, therefore,

$$\dot{\varepsilon}_r + \dot{\varepsilon}_\theta + \dot{\varepsilon}_z = 0 \tag{7}$$

where $\dot{\varepsilon}_z$ is the strain rate in the axial (z) direction.

The generalized constitutive equations for creep in an isotropic composite (Gupta *et al*. 2005), when reference frame is along the principal directions of r, θ and z are given by,

$$\dot{\varepsilon}_r = \frac{\dot{\varepsilon}_e}{2\sigma_e}[2\sigma_r - \sigma_\theta - \sigma_z] \tag{8}$$

$$\dot{\varepsilon}_\theta = \frac{\dot{\varepsilon}_e}{2\sigma_e}[2\sigma_\theta - \sigma_z - \sigma_r] \tag{9}$$

$$\dot{\varepsilon}_z = \frac{\dot{\varepsilon}_e}{2\sigma_e}[2\sigma_z - \sigma_r - \sigma_\theta] \tag{10}$$

where σ_r, σ_θ, σ_z are respectively the radial, tangential and axial stresses.

Following Von-Mises yield criterion (Dieter, 1988), the effective stress is given by,

$$\sigma_e = \frac{1}{\sqrt{2}}[(\sigma_\theta - \sigma_z)^2 + (\sigma_z - \sigma_r)^2 + (\sigma_r - \sigma_\theta)^2]^{1/2} \tag{11}$$

In a cylinder made of incompressible material with closed end, the plane strain condition exist *i.e.* the axial strain rate $(\dot{\varepsilon}_z)$ is zero (Popov 2001). Therefore, Eqs. (3), (4) and (7) on simplifying yields,

$$\dot{u}_r = \frac{C}{r} \tag{12}$$

where C is the constant of integration.

Substituting Eq. (12) into Eqs. (3) and (4), we get

$$\dot{\varepsilon}_r = -\frac{C}{r^2} \tag{13}$$

$$\dot{\varepsilon}_\theta = \frac{C}{r^2} \tag{14}$$

Under the assumption of plane strain condition ie. $\dot{\varepsilon}_z = 0$, the Eq. (10) becomes,

$$\sigma_z = \frac{\sigma_r + \sigma_\theta}{2} \tag{15}$$

Using Eq. (15) into Eq. (11), one gets

$$\sigma_e = \frac{\sqrt{3}}{2}(\sigma_\theta - \sigma_r) \tag{16}$$

Substituting Eqs. (13) and (15) into Eq. (8) we get,

$$\sigma_\theta - \sigma_r = \frac{4}{3}\left(\frac{\sigma_e C}{\dot{\varepsilon}_e r^2}\right) \tag{17}$$

Putting $\dot{\varepsilon}_e$ and σ_e respectively from Eqs. (2) and (16) in the above equation and simplifying, one gets,

$$\sigma_\theta - \sigma_r = \frac{I_1}{r^{2/n}} + I_2 \tag{18}$$

where,

$$I_1 = \left[\frac{4}{3}\right]^{\frac{n+1}{2n}} \cdot \left(\frac{C^{1/n}}{M}\right)$$

and,

$$I_2 = \frac{2}{\sqrt{3}}\sigma_o$$

On substituting Eq. (18) into equilibrium Eq. (6) and integrating, we get,

$$\sigma_r = -\frac{n}{2} \cdot \frac{I_1}{r^{2/n}} + I_2 \ln r + C_1 \tag{19}$$

where C_1 is another constant of integration.

The boundary conditions for a cylinder subjected to only internal pressure are given as,

(i) At $r = a$, $\sigma_r = -P$ (negative sign implies compressive stress) (20)

(ii) At $r = b$, $\sigma_r = 0$ (21)

Applying boundary conditions stated above, in Eq. (19), we get,

$$C_1 = \frac{nI_1}{2b^{2/n}} - I_2 \ln b$$

$$I_1 = \frac{2}{n}\frac{\left[p + I_2 \ln(a/b)\right]}{(a^{-2/n} - b^{-2/n})}$$

The values C_1 and I_1, thus obtained, are substituted in Eq. (19) to get the radial stress, σ_r,

$$\sigma_r = X\left[b^{-2/n} - r^{-2/n}\right] + I_2 \ln(r/b) \tag{22}$$

where,

$$X = \frac{\left[p + I_2 \ln(a/b)\right]}{(a^{-2/n} - b^{-2/n})}$$

Using Eq. (22) in Eq. (18), the tangential stress, σ_θ, is obtained,

$$\sigma_\theta = X\left[\left(\frac{2}{n} - 1\right) \cdot r^{-2/n} + b^{-2/n}\right] + I_2 \cdot \left(\ln\frac{r}{b} + 1\right) \tag{23}$$

Substituting Eqs. (22) and (23) in Eq. (15), we get the axial stress, σ_z,

$$\sigma_z = X\left[b^{-2/n} - r^{-2/n} + \frac{1}{n} \cdot r^{-2/n}\right] + I_2 \cdot \left[\ln\frac{r}{b} + \frac{1}{2}\right] \tag{24}$$

Based on the analysis presented, a computer program has been developed to calculate the steady state creep response of the composite cylinder for various combinations of size and content of the reinforcement (SiC_P), and operating temperature. For the purpose of numerical computation, the inner and outer radii of the cylinder are taken 25.4 *mm* and 50.8 *mm* respectively, and the internal pressure is assumed to be 85.25 *MPa*. The dimensions of cylinder and the operating pressure chosen in this study are similar to those used in earlier work (Johnson *et al*. 1961) on thick walled aluminum alloy (RR59) cylinder. The radial, tangential and axial stresses at different radial locations of the cylinder are calculated respectively from Eqs. (22), (23) and (24). The distributions of radial and tangential strain rates are computed from Eqs. (8) and (9) respectively. The creep parameters M and σ_o required during the computation process are taken from Table-1 for the desired combination of particle size, particle content and operating temperature.

5. Results and Discussions

Before discussing the results obtained in the present study, it is necessary to check the accuracy of analysis carried out and the computer program developed. To accomplish this task, following present analysis, the tangential, radial and axial stresses have been computed for a copper cylinder, for which the results are available in the literature (Johnson *et al*. 1961). The dimensions of the cylinder, operating pressure and temperature, and the values of creep parameters used for the purpose of validation are summarized in Table-2. To estimate the parameters M and σ_o for copper cylinder, firstly the values of σ_e have been calculated at inner and outer radii of cylinder by substituting in Eq. (11) the values of σ_e, σ_r, σ_θ and σ_z at these locations as reported in the study of (Johnson *et al*. 1961). The values of stresses σ_r, σ_θ and σ_z and the tangential strain rates (ε_θ) reported in reference (Johnson *et al*. (1961) at inner and outer radii are substituted in Eqn. (9) to estimate the effective strain rates (ε_e) at the corresponding radial locations. The effective stresses and effective strain rates estimated at the inner ($\varepsilon_e = 189.83\ MPa$ and $\varepsilon_e = 2.168 \times 10^{-8}\ s^{-1}$) and the outer ($\varepsilon_e = 116\ MPa$ and $\varepsilon_e = 1.128 \times 10^{-9}\ s^{-1}$) radii of the copper cylinder are substituted in creep law, Eq. (2), to estimate the creep parameters M and σ_o for copper, Table-2. The creep parameters have been used in the developed software to compute the distribution of tangential strain rate in the copper cylinder. The tangential strain rates thus obtained have been compared with those reported by (Johnson *et al*. 1961). A nice agreement is observed in Fig. 3, therefore verifying the accuracy of analysis presented and software developed in the current study.

Table 2. Summary of data used for validation

Cylinder Material : Copper
Cylinder dimensions: a = 25.4 *mm*, b =50.8 *mm*.
Internal Pressure = 23.25 *MPa*, External Pressure = 0
Operating Temperature = 250 ^0C
Creep parame ters estimated: $M = 3.271\times10^{-4}\ s^{-1/5}/MPa$,
ó$_o$ = 11.32 *MPa*

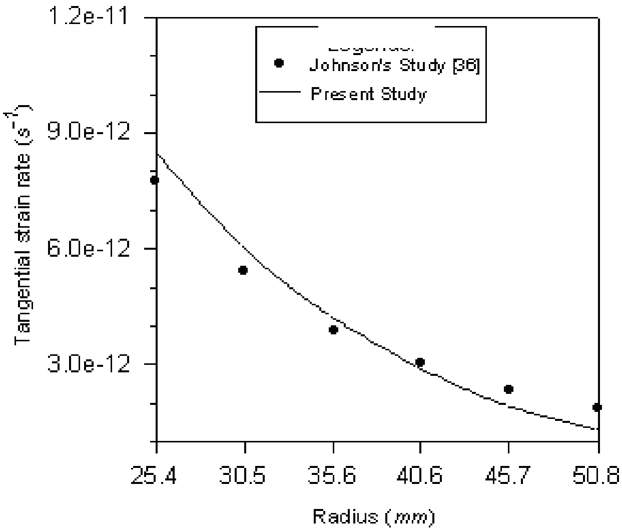

Figure 3. Comparison of tangential strain rates in copper cylinder estimated from current analysis and reported by Johnson *et al.*

5.1 Effect of Particle Size and Particle Content

Figs. 4(a)-(d) show the variation of creep stresses in composite cylinder for varying SiC_P size from 1.7 μm to 45.9 μm. The trend of stresses obtained is similar to those reported by (Bhatnagar and Arya 1974). The radial stress, Fig. 4(a), remains compressive over the entire cylinder radius with maximum at the inner radius and zero at the outer radius, due to the imposed boundary conditions given in Eqs. (20) and (21). The tangential stress shown in, Fig. 4(b), remains always tensile and increases on moving from the inner to the outer radius of cylinder. Unlike radial and tangential stresses, the axial stress, Figs. 4(c), decreases from maximum compressive, observed at the inner radius, to reach a maximum tensile value at the outer radius of the cylinder. It is clearly evident from Figs. 4(a)-(c) that the variation in particle size does not have a sizable effect on the stresses. The maximum variation observed in radial and tangential stresses are less than 1% and for axial stress it is around 5% at a radius of 30.5 *mm*, in cylinders having relatively coarser SiC_P of size 14.5 and 45.9 μm. when compared to cylinder having finer SiC_P of 1.7 μm size. The variation of effective stress, σ_e, given by Eq. (11), for varying particle size of SiC is shown in Fig. 4(d). The effective stress shown does not change on varying the particle size near the inner radius; however, towards the outer radius it decreases

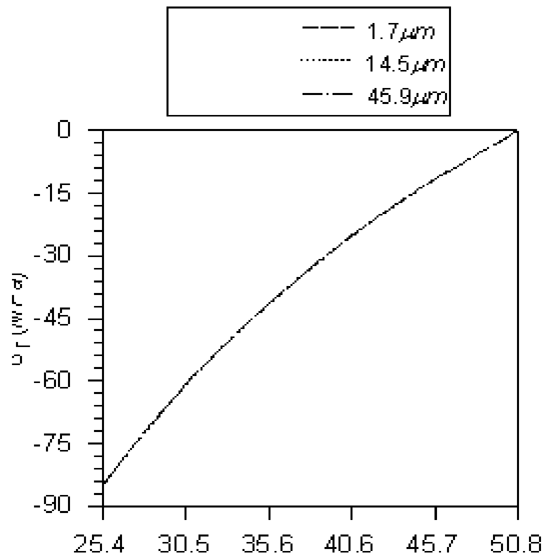

r (mm) **(4a)**

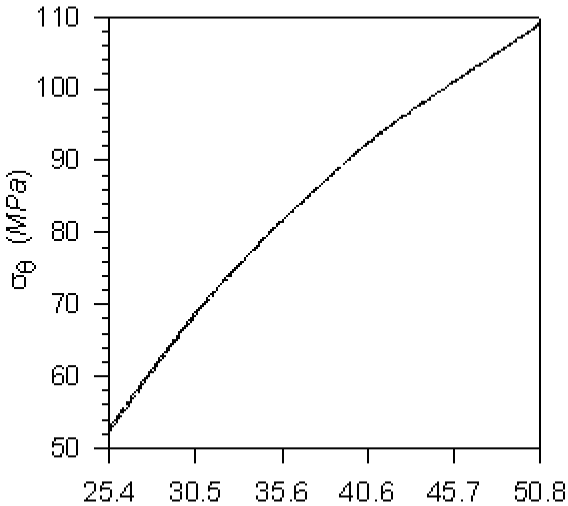

r (mm) **(4b)**

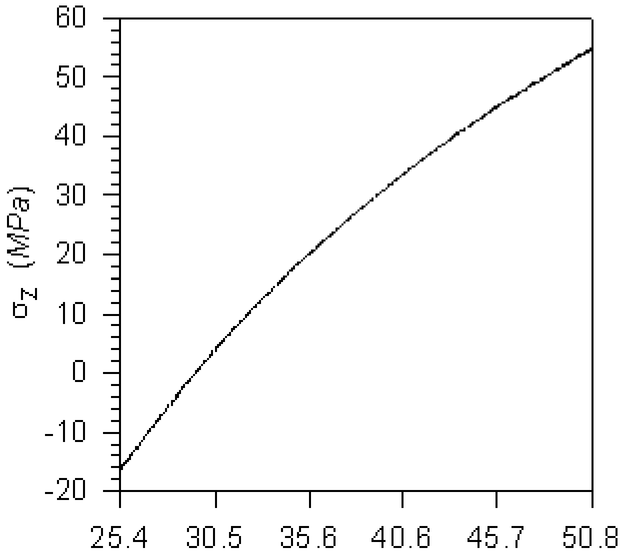

r (mm) **(4c)**

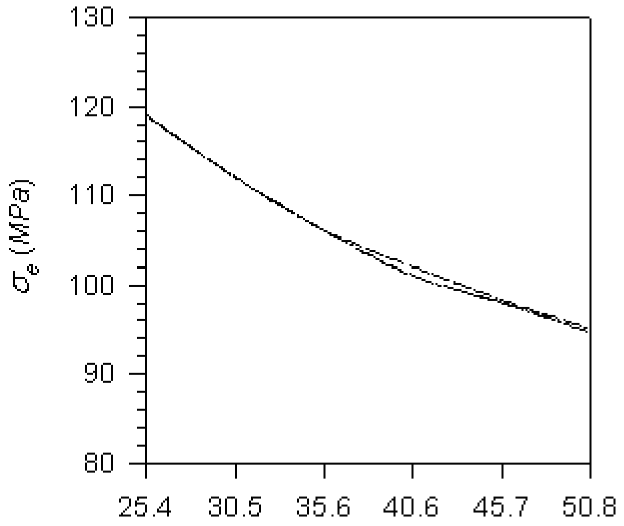

r (mm) **(4d)**

Figure 4. Variation of creep stresses in composite cylinder for varying particle size of SiC (*V = 10 vol%, T = 350ºC*)

marginally with increasing particle size. The maximum decrease of about 1% is observed at a radius 40.6 *mm* in cylinders containing relatively coarser SiC_P (14.5μm and 45.9 μm) when compared to cylinder having finer SiC_P of 1.7μm size.

The strain rates given by Eqs. (8) and (9) are related to the effective strain rate, ε_e, which ultimately depends upon (σ_e - σ_o), as evident from creep law given by Eq. (2). Therefore, to investigate the effect of particle (SiC_p) size on the creep rates, the distribution of (σ_e - σ_o), is plotted in Fig. 5. Though, the effective stress varies a little with particle size but the threshold, σ_o, decreases from 19.83 *MPa* to 16.29 *MPa* with the increase in particle size from 1.7μm to 45.9 μm, Table 1. Under external load, as the deformation of material reaches to threshold value, the interfacial debonding occurs between particles (SiC_p) and the matrix (Al) (Chen *et al*. 2008). Due to which the stress triaxiality in the matrix near the reinforcement will decrease and the debonded particles are no longer be able to transfer the stress. The damage dissipation caused by interfacial debonding increases with increase in particle (SiC_p) size (Chen *et al*. 2007), thereby decreasing the threshold stress, Table 1. As a result of this, the stress difference (σ_e - σ_o) exhibits sizable variation throughout the cylinder with decreasing SiC_P size from 45.9 μm to 1.7μm. The decrease observed towards the inner radius are relatively more than those observed near the outer radius.

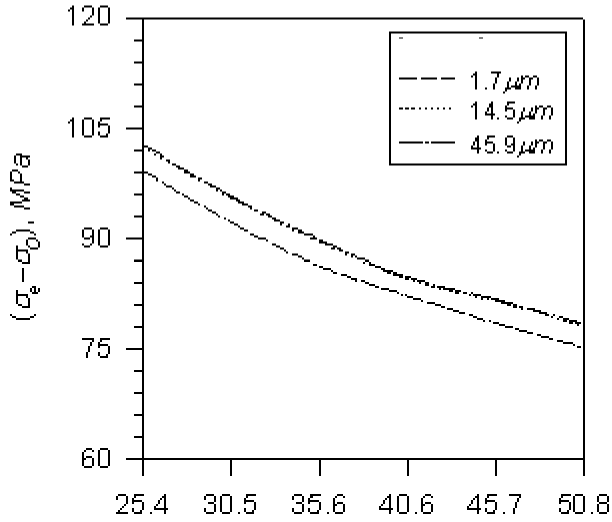

r (mm)

Figure 5. Variation of stress difference in composite cylinder for varying particle size of SiC (*V = 10 vol%, T = 350ºC*)

As a consequence, the effective strain rate (ε_e) also decreases significantly with decreasing SiC_P size as shown in Fig. 6(a). The decrease observed is about two orders of magnitude on decreasing SiC_P size from 45.9μm to 1.7 μm. The decrease in effective strain rate may be attributed to decrease in creep parameter *M* and increase in threshold stress σ_o with decreasing size of SiC_P reinforcement (Table-1) as evident from creep law given in Eq. (2). The radial (compressive) and tangential (tensile) strain rates, Fig. 6(b), decrease on moving from the inner to the outer radius of the cylinder. Throughout the cylinder, the radial and tangential strain rates remain equal in magnitude but have opposite nature due to the condition of incompressibility (Eq. 7) and of plane strain condition ($\varepsilon_z = 0$). The effect of particle size on both the strain rates is similar to those observed for effective strain rate in Fig. 6(a). The tangential and radial creep rates in the cylinder may be reduced to a significant extent by reinforcing finer SiC_P particles. The smaller size particles will be larger in number for the same volume fraction of reinforcement, thereby, leading to: (i) more transfer of load to the reinforcement with a corresponding reduction in the level of effective stress acting on the matrix, and (ii) enhancement of substructure strength, which help in restraining the

The Journal of Engineering Research Vol. 6, No. 2 (2009) 20-32

creep flow (Li and Langdon, 1998; Peng *et al*. 1998; Peng *et al*. 1999; Han and Langdon, 2002). Further, the threshold stress observed for finer particles is higher than those observed for coarser one (Table 1) due to lesser degree of debonding between particles and matrix (Chen *et al*. 2007). As a result, the load is effectively transferred from the matrix to reinforcement hence reducing the creep rates in cylinder having finer sized SiC_p.

Figures 7(a) to 7(c) show respectively the variation of radial, tangential and axial stresses in composite cylinder containing different SiC_P content *ie*. 10%, 20% and 30% by volume. The radial stress as shown in Fig. 7(a) does not vary on changing the content of SiC_P except for a small variation noticed in the middle of cylinder. Unlike particle size, the increase in particle content leads to some sizable

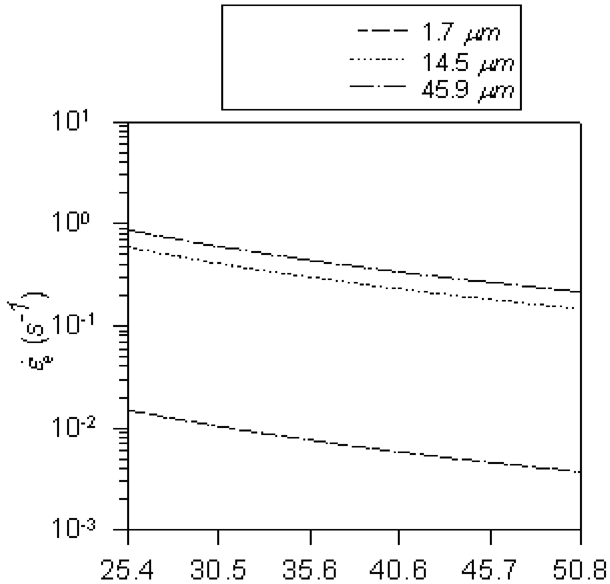

r (mm) **(6a)**

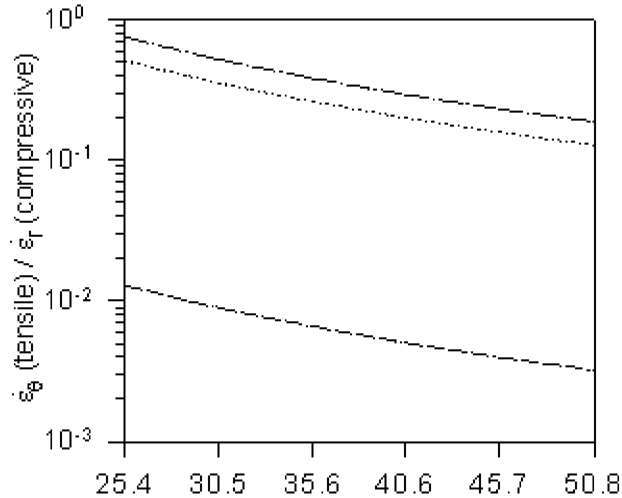

r (mm) **(6b)**

Figure 6. Variation of strain rates in composite cylinder for varying particle size of SiC (*V = 10 vol%, T = 350°C*).

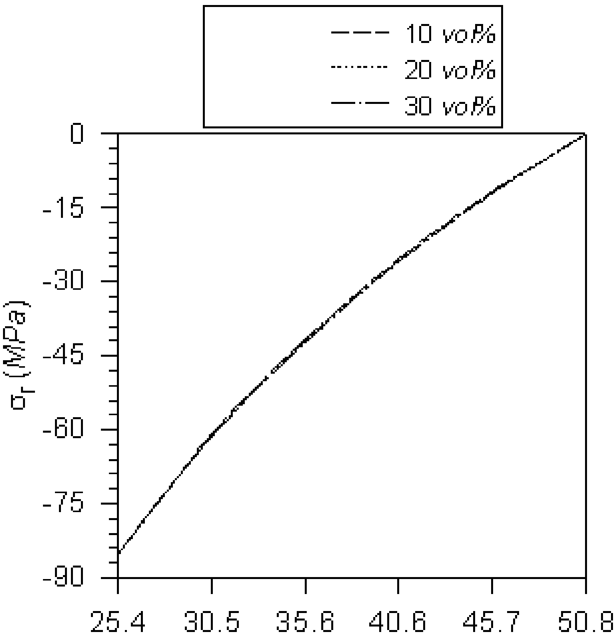

r (mm) **(7a)**

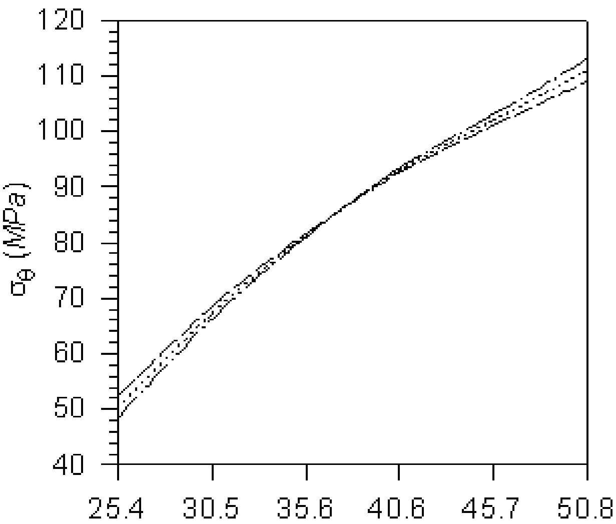

r (mm) **(7b)**

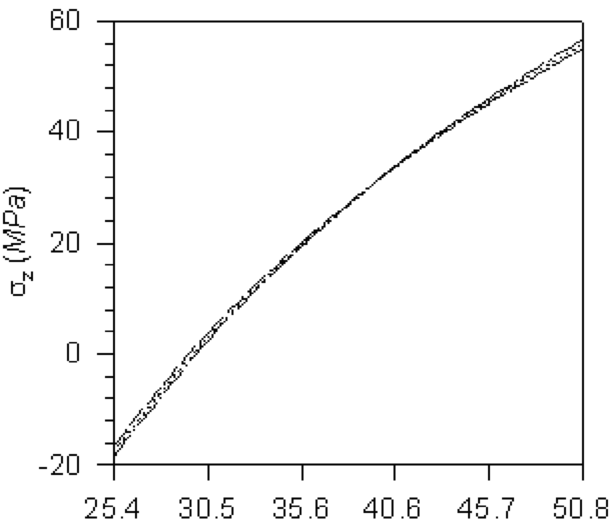

r (mm) **(7c)**

The Journal of Engineering Research Vol. 6, No. 2 (2009) 20-32

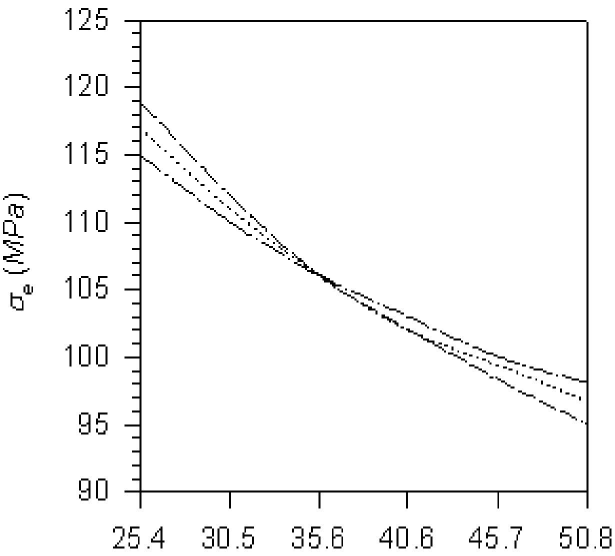

r (mm) **(7d)**

Figure 7. Variation of creep stresses in composite cylinder for varying particle content of SiC (*P = 1.7 μm, T = 350° C*)

variation in tangential and axial stresses as shown respectively in Figs. 7(b) and 7(c). On decreasing the content of SiC_P from 30% to 10%, the tangential stress increases near the inner radius but decreases towards the outer radius of the cylinder. The maximum increase and decrease observed in tangential stress are about 8% and 3.5% respectively at the inner and outer radii of the cylinder. Similar to tangential stress, the tensile values of axial stress as observed in Fig. 7(c), increases near the inner radius but decreases towards the outer radius of the cylinder on decreasing the content of SiC_P from 30% to 10%. However, at the inner radius, the compressive axial stress decreases by about 10% on decreasing the particle content from 30% to 10%. Therefore, by incorporating more amounts of reinforcement (SiC_P), the tangential and axial (only tensile values) stresses increases near the inner radius but decreases near the outer radius. The effect of particle content on effective stress, Fig. 7(d), is similar to those observed for tangential stress in Fig. 7(b). The stress difference, (σ_e - σ_o), shown in Fig. (8), decreases significantly over the entire radii with increasing SiC_P content. The decrease observed is relatively more prominent towards the inner radius compared to those observed around the outer radius. As expected, the effective strain rate decreases significantly with increasing content of SiC_P, Fig. 9 (a). The effective strain rate reduces by about two orders of magnitude on increasing the content of SiC_P from 10% to 30%. The reduction in effective strain rate, given by Eq. (2), may be attributed to decrease in creep parameter *M* and increase in threshold stress σ_o with increasing content of SiC_P (Table-1). The impact of particle content on tangential and radial creep rates, Fig. 9(b), is similar to those observed for effective strain in Fig. 9(a).

By increasing the content of SiC_P in the composite cylinder, the inter-particle spacing decreases which cause the increase in threshold stress (Li and Langdon, 1999) but decrease in creep parameter *M* (Table-1), both these factors contribute in reducing the strain rates significantly. Mishra and Pandey (1990), in their review of uniaxial creep data of Nieh (1984), have also observed that the creep rate in SiC (whisker) reinforced aluminum alloy (6061Al) composite could be reduced significantly by increasing the content of reinforcement. Similar effect of increasing SiC (particle) content on strain rate has been observed by (Pandey *et al*. 1992) for Al- SiC_P composite under uniaxial test.

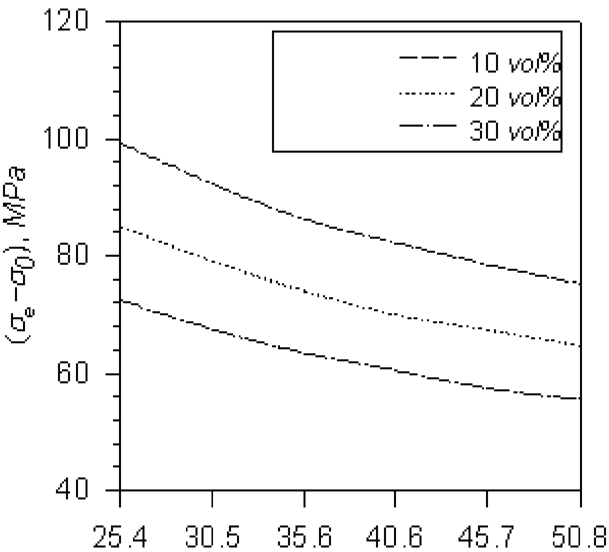

r (mm)

Figure 8. Variation of stress difference in composite cylinder for varying particle content of SiC (*P = 1.7 μm, T = 350 °C*)

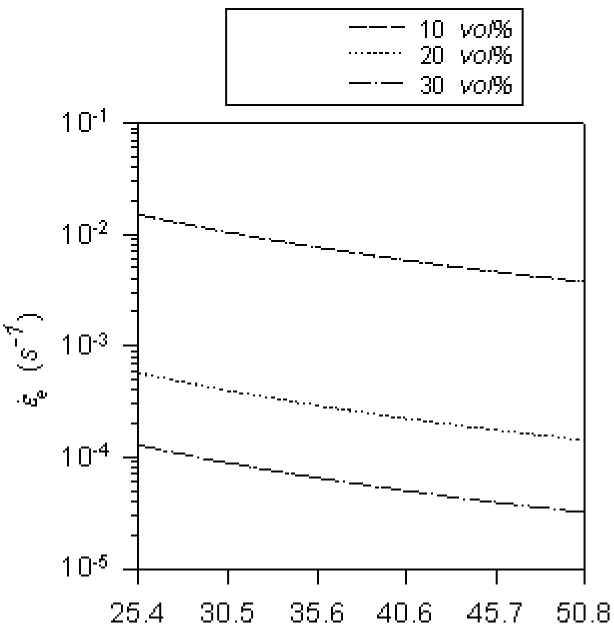

r (mm) **(9a)**

The Journal of Engineering Research Vol. 6, No. 2 (2009) 20-32

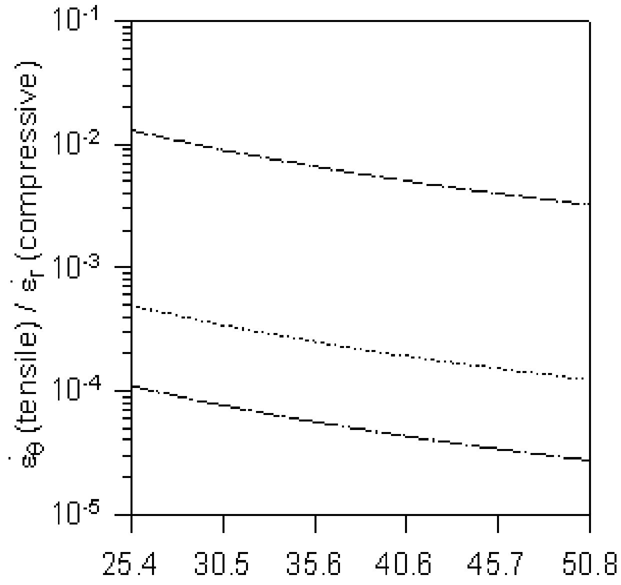

r (mm) **(9b)**

Figure 9. Variation of strain rates in composite cylinder for varying particle content of SiC (P = 1.7 μm, T = 350^{o}C)

5.2 Effect of Temperature

The creep in any material is significantly affected by operating temperature. Therefore, this section discusses the effect of varying operating temperature on the stresses and strain rates in a thick cylinder made of aluminium matrix composite containing 20 *vol%* of SiC_P. Figs. 10(a)-(c) show respectively the variation of radial, tangential, axial stresses in a composite cylinder for three different operating temperatures *ie*. 350 ^{0}C, 400 ^{0}C and 450 ^{0}C. The effect of temperature on the stresses is not significant, except for a slight variation observed in tangential stress, Fig. 10(b). On increasing the operating temperature from 350 ^{0}C to 450 ^{0}C, the tangential stress increases a little (around 1%) near the inner radius but towards the outer radius of the cylinder it does not change. The effective stress, Fig. 10(d), at the inner radius does not change with varying temperature; however, it exhibits a marginal decrease at the outer radius with increase in temperature. The stress difference, $(\sigma_e - \sigma_o)$, decreases throughout the cylinder with decreasing temperature, Fig. 11. The effective as well as radial and tangential strain rates observed in Figs. 12(a) and 12(b) respectively increases by about two orders of magnitude on increasing the temperature from 350 ^{0}C to 450 ^{0}C. With increase in operating temperature, the threshold stress σ_o decreases (Gonzalez and Sherby, 1993; Cadek *et al*. 1998) and the creep parameter M increases (Table-1), as a result of which the strain rates in the composite cylinder increase to a significant extent. The effect of temperature on the creep rate observed in this study are similar to those reported by (Pandey *et al*. 1992) for Al- SiC_P composites under uniaxial creep test.

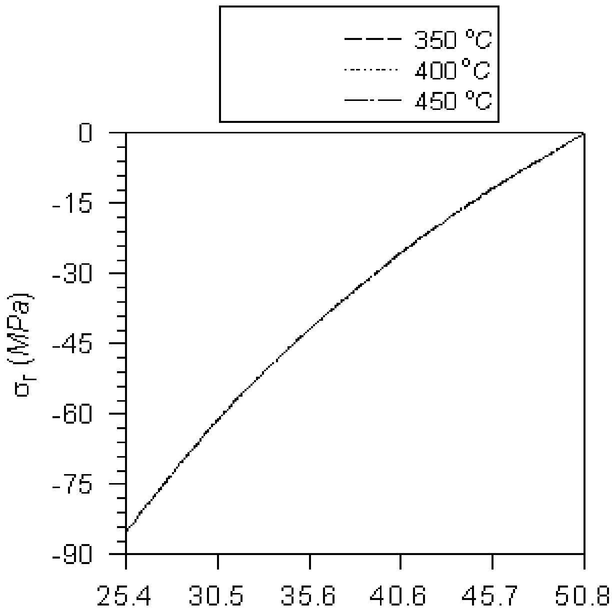

r (mm) **(10a)**

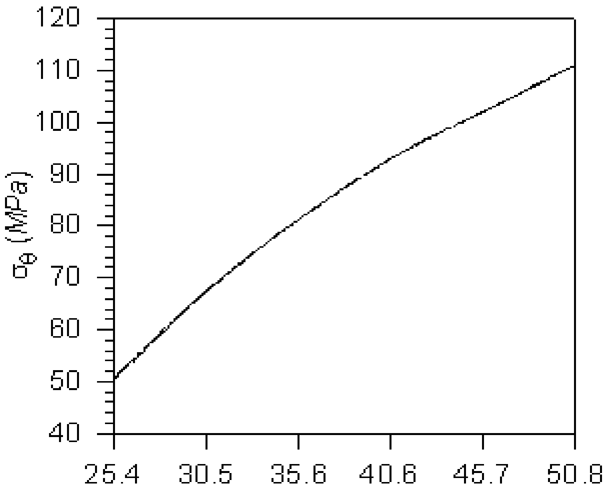

r (mm) **(10b)**

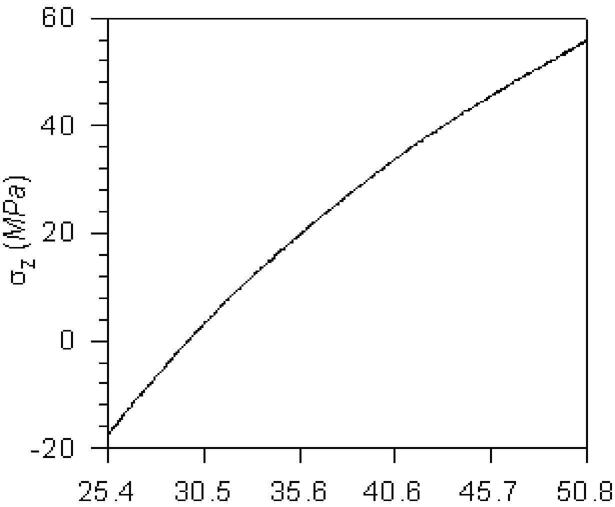

r (mm) **(10c)**

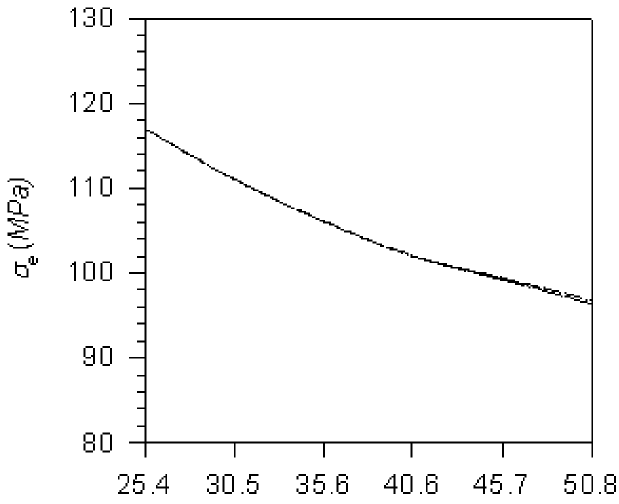

r (mm) **(10d)**

Figure 10. Variation of creep stresses in composite cylinder for varying operating temperature (*P = 1.7 μm, V = 20 vol%*)

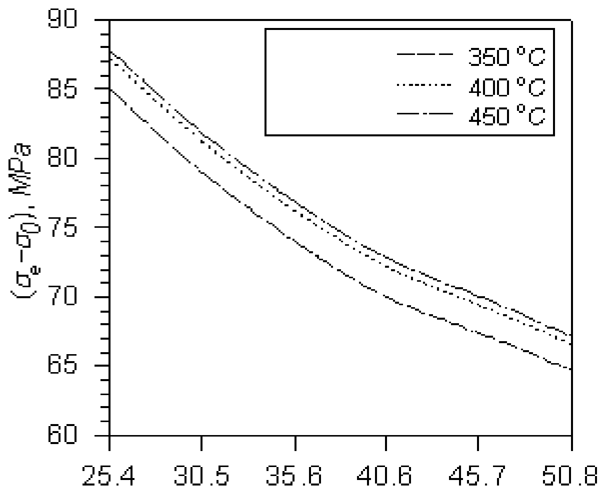

r (mm)

Figure 11. Variation of stress difference in composite cylinder for varying operating temperature (*P = 1.7 μm, V = 20 vol%*)

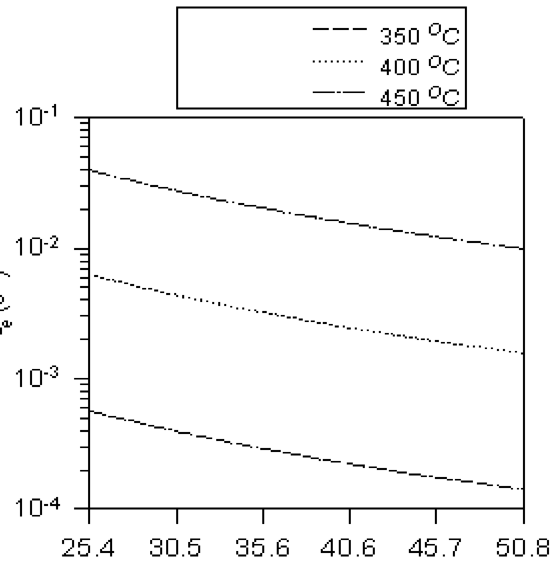

r (mm) **(12a)**

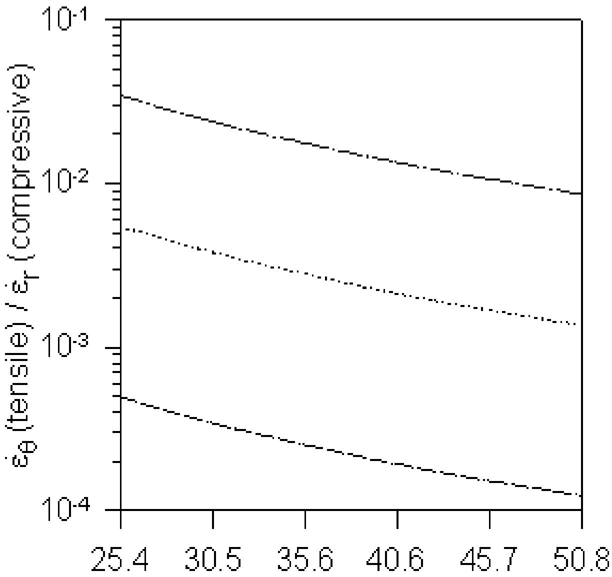

r (mm) **(12b)**

Figure 12. Variation of strain rates in composite cylinder for varying operating temperature (*P = 1.7 μm, V = 20 vol%*)

6. Conclusions

The present study has led to the following conclusions:

- The steady state radial, tangential and axial stresses increases on moving from the inner to the outer radius of a thick walled composite cylinder. The stress distributions do not vary significantly for various combinations of particle size, particle content and operating temperature, except for some sizable variation observed in tangential and axial stresses with varying content of SiC_P.
- The tangential as well as radial strain rates in an isotropic thick-wall internally pressurized Al- SiC_P cylinder decreases on moving from the inner to the outer radius. The strain rates induced in the composite cylinder could be reduced significantly by incorporating finer size of reinforcement (SiC_P), increasing the content of reinforcement and decreasing the operating temperature.

References

Abrinia, K., Naee, H., Sadeghi, F. and Djavanroodi, F., 2008, "New Analysis for the FGM Thick Cylinders under Combined Pressure and Temperature Loading," American Journal of Applied Sciences, Vol. 5(7), pp. 852-859.

Arya, V.K., Bhatnagar, N.S., 1976 "Creep of Thick Walled Orthotropic Cylinders Subjected to Combined Internal and External Pressures," J Mech Engng Sci, Vol. 18(1), pp. 1-5.

Becht IV, C. and Chen, Y., 2000, "Span Limits for Elevated Temperature Piping," ASME J Pressure

Vessel Technol, Vol. 122(2), pp. 121-124.

Bhatnagar, N.S. and Arya, V.K., 1974, "Large Strain Creep Analysis of Thick Walled Cylinder," Int J Non Linear Mechanics, Vol. 9(2), pp. 127-140.

Bhatnagar, N.S. and Gupta, S.K., 1969, " Analysis of Thick-Walled Orthotropic Cylinder in the Theory of Creep," J Physical Soc Japan Vol. 27(6), pp. 1655-1662.

Bhatnagar, N.S., Arya, V.K. and Debnath, K.K., 1980 "Creep Analysis of Orthotropic Rotating Cylinder," ASME J Pressure Vessel Technol, Vol. 102, pp. 371-377.

Buttlar, W.G, Wagoner, M, You Z. and Brovold, S.T., 2004, "Simplifying the Hollow Cylinders Tensile Test Procedure through Volume-based Strain," J. of Association of Asphalt Paving Technologies (AAPT), Vol. 73, pp 367-400.

Cadek, J., Oikawa, H. and Sustek, V., 1995, "Threshold Creep Behavior of Discontinuous Aluminium and Aluminium Alloy Matrix Composites: An Overview," Mater Sci Engng, Vol. A190(1), pp. 9-23.

Cadek, J., Pahutova, M. and Sustek, V., 1998, "Creep Behavior of a 2124 Al Alloy Reinforced by 20 vol% Silicon Carbide Particulate," Mater Sci Engng, Vol. A246(1), pp. 252-264.

Chen, J.J., Tu., S.T., Xuan, F.Z. and Wang, Z.D., 2007, "Creep Analysis for a Functionally Graded Cylinder Subjected to Internal and External Pressure," The journal of strain analysis for Engng. Design, Vol. 42(2), pp. 69-77.

Chen, J.K, Huang, Z.P. and Yuan, M.A, 2008, "Constitutive Theory of Particulate-Reinforced Viscoelastic Materials with Partially Debonded Microvoids," Computational Material Science, vol. 41, pp. 334-343.

Chen, J.K, Huang, Z.P and Zhu, J., 2007, "Size Effect of Particles on the Damage Dissipation in Nanocomposites.," Composite Science and Technology, Vol. 67, pp. 2990-2996.

Dieter, G.E., 1988, " Mechanical Metallurgy," London: McGraw-Hill.

Fukui. Y., Yamanaka, N. and Wakashima, K., 1993, "The Stresses and Strains in a Thick-Walled Tube for Functionally Graded Material under Uniform Thermal Loading," JSME , Vol. 36A(2), pp. 156-162.

Fukui, Y. and Yamanaka, N., 1992, "Elastic Analysis for Thick-Walled Tubes of Functionally Graded Material Subjected to Internal Pressure," JSME Int. J. Series I, Vol. 35(4), pp. 379-385.

Gonzalez-Doncel, G. and Sherby, O.D., 1993, "High Temperature Creep behavior of Metal Matrix Aluminium-SiC Composites," Acta Metall Mater, Vol. 4(10), pp. 2797-2805.

Gupta, VK., Singh, S.B., Chandrawat, H.N. and Ray, S., 2004, "Creep behavior of a Rotating Functionally Graded Composite Disc Operating under Thermal Gradients," Metall Mater Trans, Vol. 35A(4), pp. 1381-1391.

Gupta, V.K., Singh, S.B., Chandrawat, H.N. and Ray, S., 2005, "Modeling of Creep behavior of a Rotating Disc in presence of both Composition and Thermal Gradients," ASME J Engng Mater Technol, Vol. 127(1), pp. 97-105.

Gupta, S.K. and Pathak, S., 2001, "Thermo Creep Transition in a Thick Walled Circular Cylinder under Internal Pressure," Indian J Pure Appl Math, Vol. 32(2), pp. 237-253.

Hagihara, S. and Miyazaki, N., 2008, "Finite Element Analysis for Creep Failure of Coolant Pipe in Light Water Reactor due to Local Heating under Severe Accident Condition," Nuclear Engng Design, Vol. 238(1), pp. 33-40.

Han, B.Q. and Langdon, T.G., 2002, "Factors Contributing to Creep Strengthening in Discontinuously-Reinforced Materials," Mater Sci Engng, Vol. A322(1), pp. 73-78.

Johnson, A.E., Henderson, J. and Khan, B., 1961, "Behavior of Metallic Thick-Walled Cylindrical Vessels or Tubes Subjected to High Internal or External Pressures at Elevated Temperatures," Proc Instn Mech Engrs, Vol. 175(25), pp. 1043-1069.

King, R.H and Mackie W.W., 1967, "Creep of Thick-Walled Cylinders," ASME J Basic Engng, Vol. 89(4), pp. 877-884.

Lagneborg, R. and Bergman, B., 1976, "The Stress/Creep behavior of Precipitation-Hardened Alloys," Metal Sci Vol. 10(1), pp. 20-28.

Li, Y. and Langdon, T.G., 1998, "A Comparison of the Creep Properties of an Al-6092 Composite and the Unreinforced Matrix Alloy," Metall Mater Trans, Vol. 29A(10), pp. 2523-2531.

Li, Y. and Langdon, T.G., 1999, "An Examination of a Substructure-Invariant Model for the Creep of Metal Matrix Composites," Mater Sci Engng, Vol. A265(1), pp. 276-284.

Li, Y. and Langdon, T.G., 1997, "Creep Behavior of an Al-6061 Metal Matrix Composite Reinforced with Alumina Particulates," Acta Mater, Vol. 45(11), pp. 4797-4806.

Li, Y. and Langdon, T.G., 1999, "Fundamental Aspects of Creep in Metal Matrix Composites," Metall Mater Trans, Vol. 30A(2), pp. 315-324.

Li, Y. and Mohamed, F.A., 1997, "An Investigation of Creep Behavior in an SiC-2124 Al Composite," Acta Mater, 1997;45(11):4775-4785.

Ma, Z.Y. and Tjong, S.C., 2001, "Creep Deformation Characteristics of Discontinuously Reinforced Aluminium-Matrix Composites," Composites Sci Technol, Vol. 61(5), pp. 771-786.

Mishra, R.S. and Pandey, A.B., 1990, "Some Observations on the High-Temperature Creep Behavior of 6061 Al-SiC Composites," Metall Trans, Vol. 21A(7), pp. 2089-2090.

Mohamed, F.A., Park, K.T. and Lavernia, E.J., 1992, "Creep Behavior of Discontinuous SiC-Al Composites," Mater Sci Engng , vol. A150(1), pp. 21-35.

Nieh, T.G., 1984, "Creep Rupture of a Silicon Carbide Reinforced Aluminium Composite," Metall Trans, Vol. 15A(1), pp. 139-145.

Pai, D.H., 1967, "Steady State Creep Analysis of thick Walled Orthotropic Cylinders," Int J Mech Sci, Vol. 9(6), pp. 335-348.

Pandey, A.B., Mishra, R.S. and Mahajan, Y.R., 1994, "High-Temperature Creep of Al-TiB2 Particulate Composites," Mater Sci Engng, Vol. A189(1-2), pp. 95-104.

Pandey, A.B., Mishra, R.S. and Mahajan, Y.R., 1992, "Steady State Creep Behavior of Silicon Carbide Particulate Reinforced Aluminium Composites," Acta Metall Mater, Vol. 40(8), pp. 2045-2052.

Park, K.T., Lavernia, E.J. and Mohamed, F.A., 1990, "High Temperature Creep of Silicon Carbide Particulate Reinforced Aluminum," Acta Metall Mater, Vol. 38(11), pp. 2149-2159.

Park, K.T. and Mohamed, F.A., 1995, "Creep Strengthening in a Discontinuous SiC-Al Composite," Metall Trans, Vol. 26A(12), pp. 3119-3129.

Peng, L.M., Zhu, S.J., Ma, Z.Y., Bi, J., Chen, H.R. and Wang, F.G., 1998, " Creep Behavior in an Al-Fe-V-Si Alloy and SiC Whisker-Reinforced Al-Fe-V-Si composite," J Mater Sci, Vol. 33(23), pp. 5643-5652.

Peng, L.M., Zhu, S.J., Ma, Z.Y., Bi, J., Wang, F.G., Chen, H.R. and Northwood, D.O., 1999, "High Temperature Creep Deformation of Al18B4O33 Whisker-Reinforced 8009Al Composite," Mater Sci Engng, Vol. A265(1), pp. 63-70.

Perry, J. and Aboudi, J., 2003, "Elasto-Plastic Stresses in Thick Walled Cylinders," ASME J Pressure Vessel Technol , Vol. 125(3), pp. 248-252.

Popov, E.P., 2001, "Engineering Mechanics of Solids," Singapore: Pearson Education.

Rimrott, F.P.J., 1959, "Creep of Thick-Walled Tubes under Internal Pressure Considering Large Strains, J Appl Mech , Vol. 26, pp. 271-274.

Roy, A.K. and Tsai, S.W., 1988, "Design of Thick Composite Cylinders," ASME J Pressure Vessel Technol, Vol. 110(3), pp. 255-261.

Salzar, R.S., Pindera, M.J. and Barton, F.W., 1996, "Elastoplastic Analysis of Layered Metal Matrix Composite Cylinders-Part 1: Theory.," ASME J Pressure Vessel Technol, Vol. 118(1), pp. 13-20.

Tachibana, Y. and Iyoku, T., 2004, "Structural Design of High Temperature Metallic Components," Nuclear Engng Design, Vol. 233(1-3), pp. 261-272.

Tjong, S.C. and Ma, Z.Y., 2000, " Microstructural and Mechanical Characteristics of in Situ Metal Matrix Composites," Mater Sci Engng, Vol. R29(3-4), pp. 49-113.

Weir, C.D., 1957, "The Creep of Thick-Walled Tube under Internal Pressure," J Appl Mech, Vol. 24, pp. 464-466.

Yoshioka, H., Suzumura, Y., Cadek, J., Zhu, S.J. and Milicka, K., 1998, "Creep Behavior of ODS Aluminium Reinforced by Silicon Carbide Particulates: ODS Al-30 SiCP Composite," Mater Sci Engng , Vol. A248(1), pp. 65-72.

You, L.H., Ou H. and Zheng, Z.Y., 2007, "Creep Deformations and Stresses in Thick-Walled Cylindrical Vessels of Functionally Graded Materials Subjected to Internal Pressure," Composite Structures, Vol. 78, pp. 285-291.

You, Z. and Buttlar, W.G., 2005, "Application of Discrete Element Modeling Techniques to Predict Complex Modulus of Asphalt-Aggregate Hollow Cylinders subjected to Internal Pressure," J. of Transportation Research Board, Vol. 1929, pp. 218-226.